TRANSIENTS OF RESISTANCE-TERMINATED DISSIPATIVE LOW-PASS AND HIGH-PASS ELECTRIC WAVE FILTERS

By Wentworth Chu and Chung-Kwei Chang

Department of Physics National University of Peking

(*Received September 10, 1936*)

ABSTRACT

Formulas are derived for the solution of the transient currents of resistance-terminated dissipative π-type low-pass, T- and π-type high-pass electric wave filters. Oscillograms taken by cathode ray oscillograph for d-c. and a-c. cases are found to agree with the results calculated from these formulas. From these calculations, the following conclusions are derived: (1) When the terminating resistance is gradually increased from 0, the damping constants of the damped sine terms begin to differ greatly from each other, ranging in decreasing magnitudes from the first damped sine term to the last term of cut-off frequency. Hence the transient is ultimately of the cut-off frequency. At the cut-off frequency, this constant is greater than the corresponding constant ($R/2L$) when the termination is absent. (2) For each increase of one section, there is introduced an additional damped sine term with smaller damping constants. Therefore transients die out faster in filters of small no. of sections. (3) With the same network constants, the damping constants of π-type filters are greater than the corresponding values of T-type filters. As a result, transients die out faster in π-type filters. (4) The amplitudes of the transient terms in the attenuation and transmission ranges are of the same order of magnitude, and the filtering property only exists in the steady states. (5) The cut-off frequency of the π-type filters varies with the no. of sections used. When only two sections of low, or, high-pass filter are used, the variation amounts to nearly 26 per cent from the theoretical value.

IN a previous article, the transients of low-pass T-type filters were studied. This paper is continued from the last one and deals with the transients of π-type low-pass, and T- and π-type high-pass filters.

Derivation of formulas and calculation of transient currents

In the following discussion, let P = generalized angular velocity, and $\lambda = \sqrt{CLP}$.

1. π-type Low-pass filters: In fig. 1, let $2L$ = total inductance per section, $2R$ = total resistance of the inductance $2L = 2K_R\sqrt{L/C}$, C = capacity per section, r = resistance of $C = K_r\sqrt{L/C}$, R_0 = terminating resistance $= K_{R_0}\sqrt{L/C}$, where K_R, K_r and K_{R_0} are constants.

$$Z_1 - R = Z_1 - K_R\sqrt{L/C} = LP, Z_2 - r = Z_2 - K_r\sqrt{L/C} = 1/CP,$$

and $$L/C = (Z_1 - K_R\sqrt{L/C}) \times (Z_2 - K_r\sqrt{L/C}).$$

Solving for $\sqrt{L/C}$,

$$\sqrt{L/C} = [\sqrt{K_r^2Z_1^2 + K_R^2Z_2^2 + (4 - 2K_RK_r)} - (K_rZ_1 + K_RZ_2)]/[2(1 - K_RK_r)].$$

Let θ' be the hyperbolic angle subtended by the terminating resistance R_0, then

$$\tan h\,\theta' = K_{R_0}\sqrt{\frac{L}{C}}\Big/\sqrt{\frac{4Z_1Z_2}{Z_1 + 2Z_2}} = \frac{R_0}{Z_0}.$$

Now the value of θ, the hyperbolic angle per section, is given by the same formula as in the case of T-type low-pass filters, and neglecting the terms containing K_r^2 and K_R^2,

$$\tan h\theta' = K_{R_0}[K_r \sin h\theta + K_R \cot h\frac{\theta}{2} - 2\sqrt{2 - K_RK_r}\cos h\frac{\theta}{2}]/4(K_RK_r - 1).$$

To factor the impedance function of I_R, let

$$Z_0 \sin h\,(N\theta + \theta') = 0,$$

hence

$$N\theta + \theta' = j\kappa\pi,$$

and

W. Chu and C. K. Chang, Chinese J. of Phyl, vol. 2, no. 1, pp. 76-105, (1936)

$$\tan h\, N\theta = -\tan h\theta' = \frac{K_{R_0}}{4(1-K_RK_r)}\Big[K_r \sin h\theta + K_R \cot h\,\frac{\theta}{2} -$$

$$2\sqrt{2-K_RK_r}\cos h\,\frac{\theta}{2}\Big] = \sin hN\theta/\cos hN\theta.$$

Clearing of fractions and rearranging,

$$\frac{K_{R_0}K_r}{8(1-K_RK_r)}\left[\cos h(N+1.5)\theta + \cos h(N-1.5)\theta\right] -$$

$$\left[1 - \frac{K_{R_0}(K_R - .5K_r)}{4(1-K_RK_r)}\right]\cos h(N+.5)\theta +$$

$$\left[1 + \frac{K_{R_0}(K_R - .5K_r)}{4(1-K_RK_r)}\right]\cos h(N-.5)\theta = \frac{K_{R_0}\sqrt{2-K_RK_r}}{4(1-K_RK_r)}$$

$$\left[\sin h(N+1)\theta - \sin h(N-1)\theta\right].$$

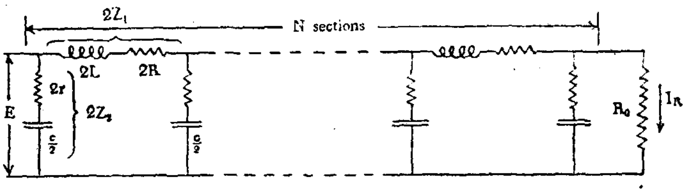

Fig. 1.

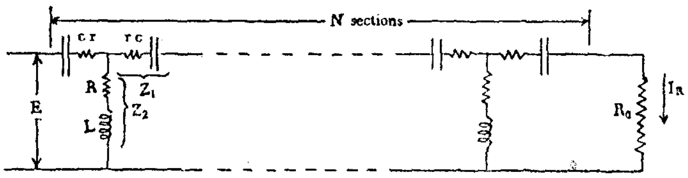

Fig. 2.

Letting $\theta = a + jb$, and equating the real and imaginery parts separately,

$$F[\cos h\,(N+1.5)\,a \cos(N+1.5)\,b + \cos h\,(N-1.5)\,a\cos(N-1.5)\,b] - (1-G)\cos h\,(N+.5)\,a\cos(N+.5)\,b + (1+G)\cos h\,(N-.5)\,a\cos(N-.5)\,b = H[\sin h\,(N+1)\,a\cos(N+1)\,b - \sin h\,(N-1)\,a\cos(N-1)\,b], \quad (1)$$

and

$F[\sin h\,(N+1.5)\,a \sin\,(N+1.5)\,b + \sin h\,(N-1.5)\,a \sin\,(N-1.5)\,b]-$
$(1-G) \sin h(N+.5)\,a \sin(N+.5)\,b + (1+G) \sin h(N-.5)\,a \sin(N-.5)\,b =$
$H[\cos h\,(N+1).a \sin\,(N+1)\,b - \cos h\,(N-1)\,a \sin\,(N-1)\,b],$ (2)

where $F = K_{R0}\,K_r/8(1-K_RK_r),\ G = K_{R0}\,(K_R - .5\,K_r)/4(1-K_RK_r),$

and $H = K_{R0}\sqrt{2-K_R\,K_r}/4(1-K_R\,K_r).$

From these two formulas, N values of θ can be found by cut-and-try method. Having found θ's, the factors of the impedance function of I_R can be found by the same formula as in the T-type filters to be of the type $1+A_1\lambda+B_1\lambda^2$, where A_1 and B_1 are constants derived from the value of θ. Now I_R can be shown by deduction to be given by $I_R = \sqrt{\frac{C}{L}}(K_r\lambda+1)^N/(2NK_R+K_{R0})\,(1+A_1\lambda+B_1\lambda^2)\,(1+A_2\lambda+B_2\lambda^2)\cdots(1+A_n\lambda+B_n\lambda^2)$ From this formula, the transients under d-c. and a-c. impressed voltages can be easily calculated, and the results are shown in Tables I and II.

[2] T-type High-pass Filters: In fig. 2, let $C/2$=capacity per section, $2r$=resistance of $C/2 = 2K_r\sqrt{\frac{L}{C}}$ L = inductance per section, and R = resistance of $L = K_R\sqrt{L/C}$, and R_0 = terminating resistance $= K_{R0}\sqrt{L/C}$, where K_r, K_R and K_{R0} are constants. Now $Z_1 - r = 1/CP$, $Z_2 - R = LP$, and $L/C = (Z_1 - K_r\sqrt{L/C})\,(Z_2 - K_R\sqrt{L/C})$. By comparing with the T-type low pass filters in the previous paper, these formulas are the same except that K_R and K_r are interchanged. Therefore the formulas for the determination of θ's can be written down as follows:

$(1+F)\cos h\,(N-1)\,a \cos\,(N-1)\,b - (1-F)\cos h\,(N+1)\,a \cos(N+1)$
$b + G \cos h\,N\,a \cos N\,b =$
$H[\sin h\,(N+.5)\,a \cos\,(N+.5)\,b - \sin h\,(N-.5)\,a \cos\,(N-.5)\,b],$ (3)

and

$(1+F)\sin h\,(N-1)\,a \sin\,(N-1)\,b - (1-F)\sin h\,(N+1)\,a \sin\,(N+1)$
$+ G \sin h\,N\,a \sin N\,b =$

$H[\cos h\,(N+.5)\,a \sin\,(N+.5)\,b - \cos h\,(N-.5)\,a \sin\,(N-.5)\,b],$ (4).,

where

$F = K_{R0}K_R/2(1-K_RK_r),\ G = K_{R0}(K_r - K_R)/(1-K_RK_r),$

and $H = K_{R0}\sqrt{2-K_RK_r}/(1-K_RK_r).$

From these two formulas, $N+1$ values of θ can be found, of which one is a negative number, and the rest are complex numbers with real parts negative. Knowing θ's, the factors of the impedance functions of I_R can be found by the same formulas as in the previous paper to be of the types $\lambda + X_0$ and $\lambda^2 + A_1\lambda + B_1$, where A_1 and B_1 are constants derived from θ. By deduction, $I_R = \sqrt{\frac{C}{L}}\,\lambda(\lambda^2 + K_R\lambda)^N / [(K_{R_0} + 2NK_r)(\lambda + X_0)(\lambda^2 + A_1\lambda + B_1)(\lambda^2 + A_2\lambda + B_2)\cdots(\lambda^2 + A_n\lambda + B_n)]$. From this formula, the transients under *d–c.* and *a–c.* voltages are calculated and shown in tables III, IV, V, VI, VII, & VIII.

[3] π-type high-pass filters: The formulas for the determination of θ's are the same as in the case [1], except that K_R and K_r are interchanged. From these formulas N values

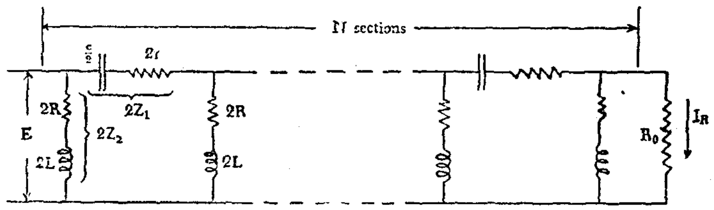

Fig. 3.

of θ can be found, and the factors are of the type $\lambda^2 + A_1\lambda + B_1$. By deduction $I_R = \sqrt{\frac{C}{L}}\,(K_R\lambda + \lambda^2)^N / [(K_{R_0} + 2NK_r)(\lambda^2 + A_1\lambda + B_1)\cdots(\lambda^2 + A_n\lambda + B_n)]$. From this formula, the transients under *d–c.* and *a–c.* impressed voltages are calculated and shown in tables IX and X.

Tables

In the following tables, $\sqrt{\dfrac{C}{L}} = I_0$, and $\dfrac{t}{\sqrt{CL}} = t'$.

Table I: 2 sections of π-type low pass filter, $K_R = .046526$, $K_r = .007172$, $K_{R_0} = \sqrt{2}$. The impressed voltage is either unit *d-c.* voltage, or $\sin(\varkappa t' + \alpha)$, and the current is of the type $I_R = I_0[A$, or $A\sin(\varkappa t' + \theta)$, $+ A_1\varepsilon^{-.5404t'}\sin(.4144t' + \theta_1) + A_2\varepsilon^{-.2133t'}\sin(1.781t' + \theta_2)]$.

$\varkappa$	*D-c.*	.964
α		325.5°
A	+.6249	−.615
θ		−.23.43°
A_1	−1.0886	+.732
θ_1	+51.698°	+25.314°
A_2	−.2605	+.634
θ_2	−61.71°	−61.878°

Table II: 5 sections of π-type low-pass filter, with conditions same as in Table I. The current is of the type $I_R = I_0 [A$, or $A \sin(\varkappa t' + \theta), + A_1 \varepsilon^{-.2762t'} \sin(.23622t' + \theta_1) + A_2 \varepsilon^{-.2756t'} \sin(.50273t' + \theta_2) + A_3 \varepsilon^{-.1528t'} \sin(.85129t' + \theta_3) + A_4 \varepsilon^{-.08286t'} \sin(1.1515t' + \theta_4) + A_5 \varepsilon^{-.0435t'} \sin(1.3465t' + \theta_5)]$.

$\varkappa$	*D-c.*	1.148
α		312.7°
A	.5321	−.413
θ		−49.06°
A_1	−1.499	+.404
θ_1	+53.443°	+8.289°
A_2	−.7894	−.364
θ_2	−85.174°	+26.518°
A_3	+.2374	+.3355
θ_3	−35.287°	+52.665°
A_4	−.06914	+.499
θ_4	−23.073°	−63.55°
A_5	+.01402	−.04767
θ_5	−18.737°	+9.122°

Table III: One section of T-type high-pass filter, $K_r = .0134$, $K_R = .030692$, $K_{R_0} = \sqrt{2}$. The impressed voltage is either unit *d-c.* voltage, or $\sin(\varkappa t' + \alpha)$, and $I_R = I_0 [A \sin(\varkappa t' + \theta) + A_0 \varepsilon^{-2.5528t'} + A_1 \varepsilon^{-.10708t'} \sin(.7225t' + \theta_1)]$.

$\varkappa$	*D−c.*	.934	.581
α		111.23°	136.2°
A		−.9775	+.2945
θ		+35.488°	−19.62°

A_0	+.5479	+.3874	+.459
A_1	−.4827	+.8526	−.79
θ_1	−17.6°	+75.573°	−8.74°

Table IV: 2 sections of T-type high-pass filter with the same constants as in Table III. $I_R = I_0 [A\sin(\varkappa t' + \theta) + A_0 \varepsilon^{-1.6119t'} + A_1 \varepsilon^{-.5646t'} \sin(1.0799t' + \theta_1) + A_2 \varepsilon^{-.04629t'} \sin(.75323t' + \theta_2)]$.

$\varkappa$	$D-c.$	.77
α		123°
A		+1.081
θ		+28.264°
A_0	+.647	+.578
A_1	−.771	−.9585
θ_1	−11.64°	−17.3°
A_2	+.139	−1.098
θ_2	−61.864°	+47.2°

Table V: 5 sections of T-type high-pass filters withe same constants as in Table III. $I_R = I_0 [A\sin(\varkappa t' + \theta) + A_0 \varepsilon^{-2.6265t'} + A_1 \varepsilon^{1.6342t'} \sin(1.9t' + \theta_1) + A_2 \varepsilon^{-.3649t'} \sin(1.3807t' + \theta_2) + A_3 \varepsilon^{-.10346t'} \sin(.975t' + \theta_3) + A_4 \varepsilon^{-.05879t'} \sin(.7898t' + \theta_4) + A_5 \varepsilon^{-.02054t'} \sin(.71548t' + \theta_5)]$.

$\varkappa$	$D—c.$	.807
α		244.6°
A		−.718
θ		−52°
A_0	+.7535	−.5312
A_1	−1.4142	+1.171
θ_1	−5.138°	−18.41
A_2	+.4164	−.4912
θ_2	−57.947°	−85.882°
A_3	−.1873	−.4775
θ_3	−68.522°	+66.556°
A_4	+.0786	+.713
θ_4	+76.356°	−32.367°
A_5	−.02222	+.08
θ_5	−79.129°	+87.455°

Table VI : 5 sections of T-type high-pass filter without termination $K_R = .030692$, $K_r = .0134$. The indicial admittance of the receiving-end is given by $A_R(t) = I_0\,[7.46\varepsilon^{-74.65t'} - .4575\varepsilon^{-.0304t'} \sin 2.283t' + .2404\varepsilon^{-.02504t'} \sin 1.201t' - .1747\varepsilon^{-.0205t'} \sin .8737t' + .149\varepsilon^{-.01905t'} \sin .7435t' - .07067\varepsilon^{-.0187t'} \sin .7074t']$.
Table VII : 5 sections of T-type high-pass filter with $K_R = K_r = 0$, and $K_{R_0} = \sqrt{2}$. The indicial admittance of the receiving-end is given by $A_R(t) = I_0[1.01\varepsilon^{-3.174t'} - 1.29\varepsilon^{-1.5t'} \sin(1.855t' + 2.806°) + .476\varepsilon^{-.3365t'} \sin(1.384t' - 47.945°) - .1887\varepsilon^{-.0818t'} \sin(.981t' - 67.673°) + .07912\varepsilon^{-.0192t'} \sin(.79t - 75.33°) - .02238\text{-}\varepsilon^{-.00175t'} \sin(.715t' - 78.232°)]$.

Table VIII : 2 sections of π-type high-pass filters of the same constants as those in Table III. $I_R = I_0[A\sin(\varkappa t' + \theta) + A_1\,\varepsilon^{-1.24t'} \sin(.9192t' + \theta_1) + A_2\,\varepsilon^{-.1797t'} \sin(.89t' + \theta_2)]$.

$\varkappa$	$D-c.$	1.0335
α		70.5°
A		−.61
θ		+60.8°
A_1	−1.1874	−.758
θ_1	−49.802°	−80.553°
A_2	−.2554	−.447
θ_2	+62.323°	−72.245°

Table IX : 5 sections of π-type high–pass filter of the same constants as those in table III. $I_R = I_0\,[A\sin(\varkappa t' + \theta) + A_1\varepsilon^{-2.444t'} \sin(1.5819t' + \theta_1) + A_2\varepsilon^{-.75257t'} \sin(1.648t' + \theta_2) + A_3\varepsilon^{-.1855t'} \sin(1.14t' + \theta_3) + A_2\varepsilon^{-.06095t'} \sin(.8638t' + \theta_4) + A_5\varepsilon^{-.02633t'} \sin(.7418t' + \theta_5)]$.

$\varkappa$	D-$c.$	1.237
α		131°
A		−.5912
θ		−62.08°
A_1	−1.602	−1.167
θ_1	−50.8°	−77.94°
A_2	−.7542	+,993
θ_2	+69.877°	−66.429°

A_3	$+.234$	$+.693$
θ_3	$+35.454°$	$-29.3°$
A_4	$-.0707$	$+.0827$
θ_4	$+23.343°$	$+87.711°$
A_5	$+.01446$	$-.01318$
θ_5	$+18.526°$	$+64.768°$

Experiment for checking some of the formulas derived

The transients were taken by a cathode-ray oscillograph, and the circuit arrangements were the same as those in the T-type low-pass filters in the last paper. In the low-pass filters, $R = 52.5$ ohms $= .046526\sqrt{L/C}$, $L = .64$ henry, $C = .50264\ \mu f.$, $r = 8.11$ ohms, $= .007172\sqrt{L/C}$, $R_o = \sqrt{2}\sqrt{L/C} = 1595.8$ ohms. In the T- and π-type high-pass filters, $C = .504\ \mu f$, $L = .32$ henry, $R = 24.456$ ohms $= .030692\sqrt{L/C}$, $r = .0134\sqrt{L/C} = 10.676$ ohms, and $R_o = 1127$ ohms $= \sqrt{2}\sqrt{L/C}$. The pictures taken were shown in Fig.'s 4-17. The calculated and experimental results were plotted side by side in Fig.'s 18-31, where the discrepancies were found to be small.

Conclusions

The formulas gave results which checked pretty well with experimental values. From calculated results as shown in tables V and VI, the effect of terminating resistance is to make the damping constants of the damped terms differ greatly from each other. Without termination, the damping constant is very nearly $R/2L$ for all the sine terms. As a result, the transients die out very slowly, and in the transient state there is no definite frequency. As the terminating resistance is gradually increased, the damping constants all increase, and differ from each other, ranging in decreasing magnitudes from the first sine term to the last sine term of the cut-off frequency. No matter what the external frequency is, the transient is ultimately of the cut-off frequency. This smallest damping constant of the cut-off term is greater than the corresponding constant when termination is absent, which is very nearly equal to $R/2L$. As the terminating resistance is increased, the deviation of the smallest damping constant from $R/2L$ is increased, and transient dies out faster.

The effect of sectional resistance R is very large on the damping constants, as their deviation due to termination is all based on $R/2L$. Thus, with $R=0$ in Table VII, the smallest damping constant is only .00175, and transient dies out very slowly.

The effect of the number of sections can be seen form data in Tables I-V, VIII and IX. For the same sectional resistance and terminating resistance, the damped terms increase with the no. of sections. With each increase of the no. of sections, there is an increase of one transient term with smaller damping constant. Hence transient dies out fa ter in a filter of smaller no. of sections. While sectional resistance and no. of sections affect damping constants considerably, they have no large effect on the transient amplitude.

From tables IV and VIII, V and IX, the corresponding damping constants of T- and π- type filters with identical circuit constants differ from each other, with those of π-type larger. Therefore transient dies out faster in π-type filters.

From data in Table III, the transient amplitudes after cut-off are of the same order of magnitudes as those inside the transmission band and the amplitudes are enormous compared with the steady-state amplitudes. Hence the ordinary steady-state filter property is entirely lost in the transient state.

From the data in Tables I, II, VIII and IX, the cut-off frequencies of π-type filters vary with the no. of sections used. When only two sections of low or high-pass filters are used, the variation is a maximum and amounts to nearly 26 per cent from the theoretical value. This variation decreases with the increase of the no. of sections.

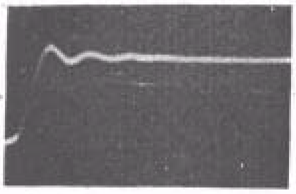

Fig. 4
Indicial admitance of the receiving-end of 2 section Low-pass π-type Filter.

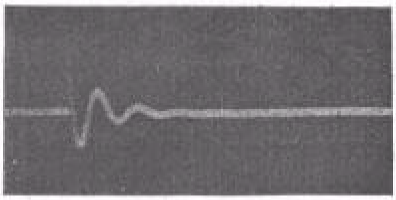

Fig. 8
Indicial admittance of the receiving-cnd of 1 section High-pass T-type Filter.

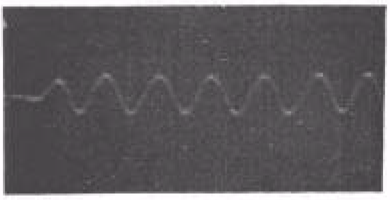

Fig. 5
$I_R(t)$ of 2 section Low-pass π-type Filter under an impressed voltage $\sin(1698.35t+325.5°)$

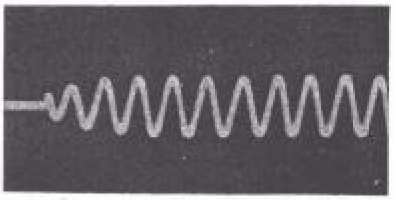

Fig. 9
$I_R(t)$ of 1 section High-pass T-type Filter under an impressed voltage $\sin(2324.8t+111.23°)$

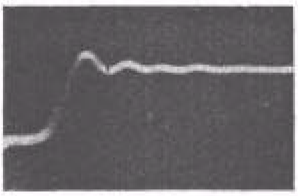

Fig. 6
Indicial admitance of the receiving-end of 5 section Low-pass π-type Filter.

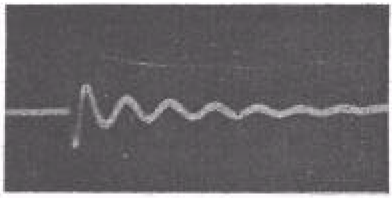

Fig. 10
Indicial admittance of the receiving-end of 2 section High-pass T-type Filter.

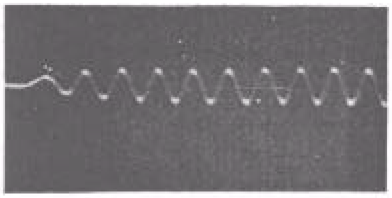

Fig 7
$I_R(t)$ of 5 section Low-pass π-type Filter under an impressed voltage $\sin(2023.2t+312.7°)$

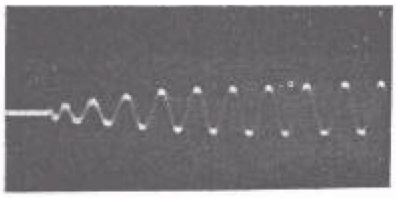

Fig. 11
$I_R(t)$ of 2 section High-pass T-type Filter under an impressed voltage $\sin(1915.12t+123°)$.

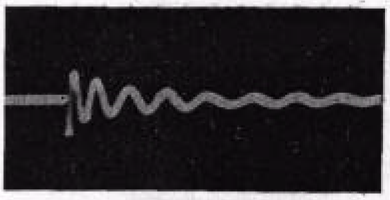

Fig. 12
Indicial admittance of the receiving-end of 5 section High-pass T-type Filter.

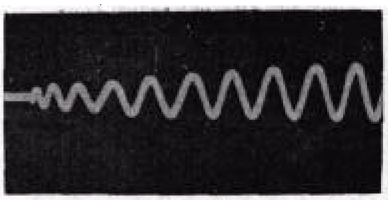

Fig. 13
$I_R(t)$ of 5 section High-pass T-type Filter under an impressed voltage $\sin(2010{\cdot}6t+244{\cdot}6^\circ)$.

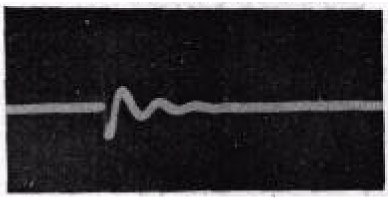

Fig. 14
Indicial admittance of the receiving-end of 2 section High-pass π-type Filter.

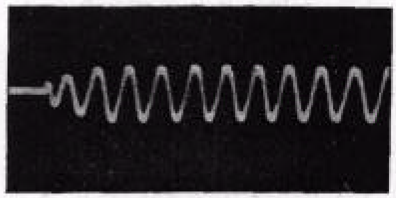

Fig. 15
$I_R(t)$ of 2 section High-pass π-type Filter under an impressed voltage $\sin(2576.1t+70.5^\circ)$

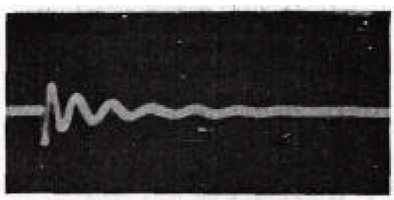

Fig. 16
Indicial admittance of the receiving-end of 5 section High-pass π-type Filter.

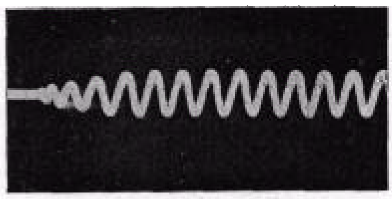

Fig. 17
$I_R(t)$ of 5 section High-pass π-type Filter under an impressed voltage $\sin(3078{\cdot}8t+131^\circ)$

In the following figures, the solid curves represent the calculated results and the dotted curves represent the experimental results.

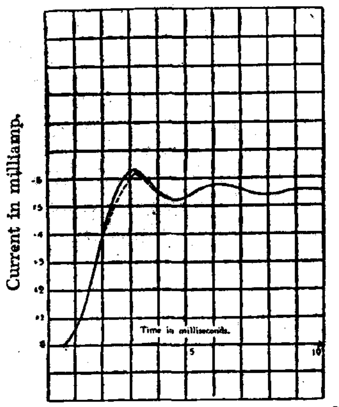

Fig. 18. Indicial Admittance of the rceivingend of 2 section Low-pass π-type Filter.

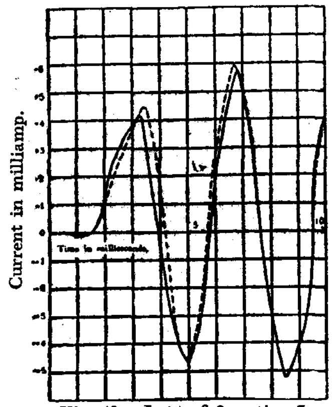

Fig. 19. $I_R(t)$ of 2 section Low-pass π-type Filter under an impressed voltage sin (1698.35t + 325·5°).

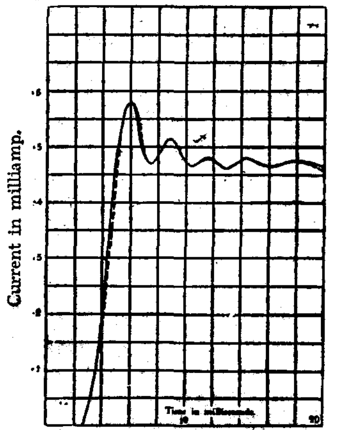

Fig. 20. Indicial Admittance of the receiving-end of 5 section Low-pass π-type Filter

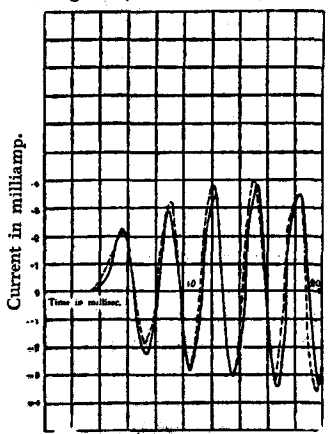

Fig. 21. $I_R(t)$ of 5 section Low-pass π-type Filter under an impressed voltage sin (2025.22t + 312.7°).

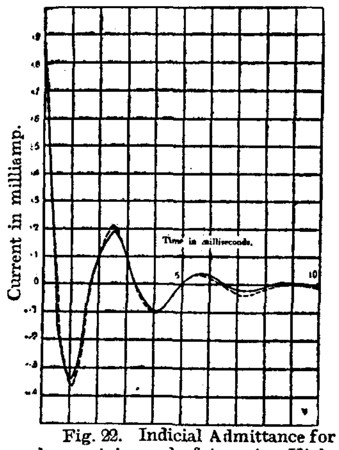

Fig. 22. Indicial Admittance for the receiving-end of 1 section High-pass T-type Filter.

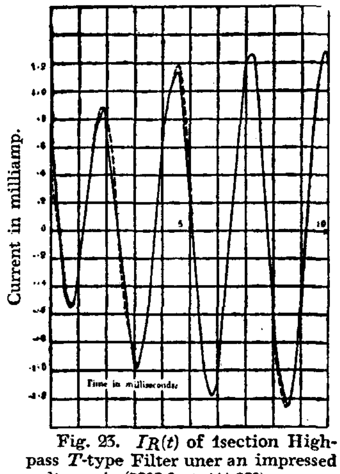

Fig. 23. $I_R(t)$ of 1section High-pass T-type Filter uner an impressed voltage sin (2323.8t + 111.23°).

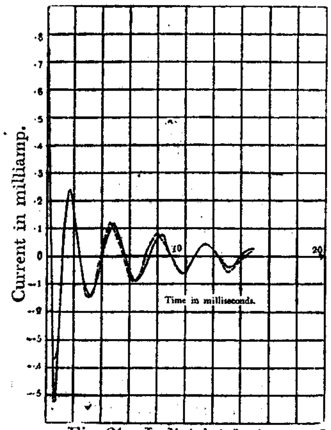

Fig. 24. Indicial Admittance for the receiving-end of 2 section High-pass T-type Filter.

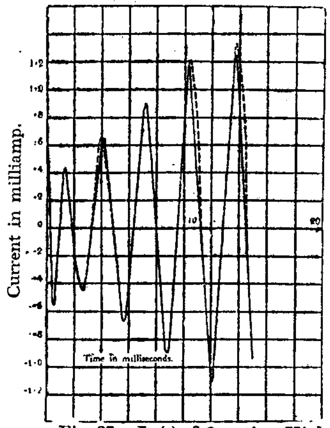

Fig. 25. $I_R(t)$ of 2 section High-pass T-type Filter under an impressed veltage sin (1915.12t + 125°).

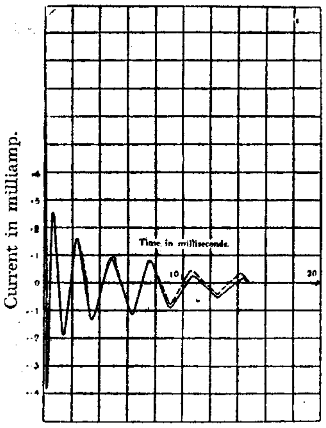

Fig. 26. Indicial Admittance of the receiving-end of 5 section High-pass T-type Filter.

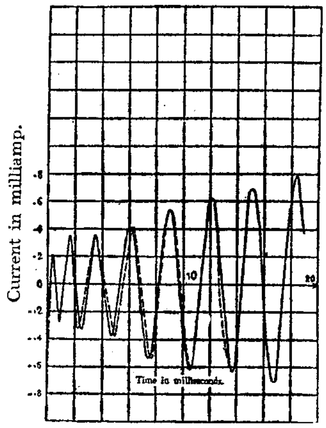

Fig. 27. $I_R(t)$ of 5 section High-pass T-type Filter under an impressed voltage sin (2010.6t + 244.6°).

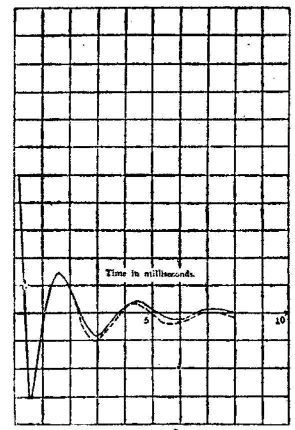

Fig. 28. Indicial Admittance of the receiving-end of 2 section High-pass π-type Filter.

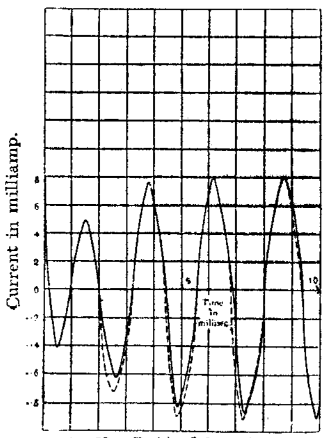

Fig. 29. $I_R(t)$ of 2 section High-pass π-type Filter under an impressed voltage sin (2576.1t + 70.5°).

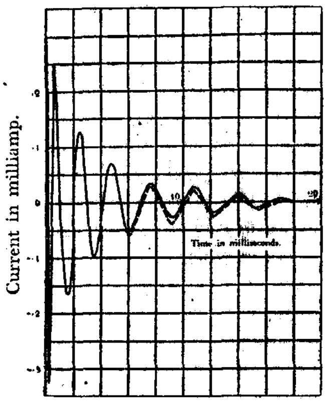

Fig. 30. Indicial Admittance of the receiving-end of 5 section High-pass π-type Filter.

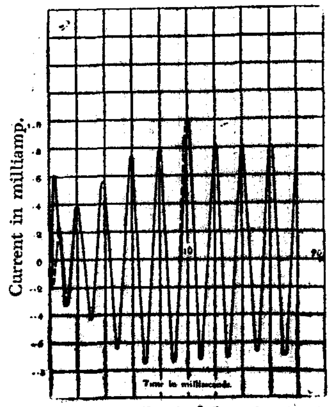

Fig. 31. $I_R(t)$ of 5 section High-pass π-type Filter under an impressed voltage $\sin(3078.8t + 131°)$.